Non-scanning, non-interferometric, three-dimensional optical profilometer with nanometer resolution

Chen-Tai Tan (譚振台), Yuan-Sheng Chan (詹遠生), Jhao-An Chen (陳昭安), Teh-Chao Liao (廖得照), and Ming-Hung Chiu (邱銘宏)*

Department of Electro-Optical Engineering, National Formosa University
No. 64, Wunhua Road, Huwei, Yunlin 632, China
**Corresponding author: mhchiu@nfu.edu.tw*

Received March 14, 2011; accepted April 28, 2011; posted online August 5, 2011

A non-scanning, non-interferometric, three-dimensional (3D) optical profilometer based on geometric optics, critical angle principle, and the use of a charge-coupled device (CCD) camera is presented. The surface profile of the test specimen can be transferred into the reflectance profile. The reflectance profile, obtained from a CCD, is the ratio of the intensity at the critical angle to the intensity obtained at the total internal reflection angle. The optical profilometer provides a sub-micron measuring range with nanometer resolution and can be used to measure roughness or surface defects in real time.

OCIS codes: 120.6660, 120.5700, 120.3940, 110.6880, 080.2468.
doi: 10.3788/COL201109.101202.

Optical profilometers may be distinguished into two types: scanning and non-scanning types. Scanning profilometers have better axial resolution but spend much time in measuring. For three-dimensional (3D) surface profile measurement, scanning approaches such as confocal microscopy[1−3], or near-field microscopy[4], which have high axial and lateral resolutions for measuring a small scanned area, are usually not used to measure a large surface profile. Non-scanning approaches such as the noninterferometric method[5,6], interference microscopy[7−10], and second-harmonic generation[11], can measure a large surface field, but the surface height calculation based on the fringe analysis is more complex.

In this letter, a new non-scanning and non-interferometric optical profilometer based on the critical angle method[12−14] and the use of a charge-coupled device (CCD) camera is proposed. The algorithm of the critical angle method transforms the surface height into the reflectance[14], and a CCD is used to measure the reflectance profile at the image plane. From the reflectance profile, two-dimensional (2D) and 3D electronic images may be obtained simultaneously. The profilometer is a useful and rapid approach for measuring a large surface profile (the whole area of the reflection beam) in one shot. The test area may be the whole size of the beam and is directly dependent on optical magnification and CCD size. In the current method, even large area measurements can be obtained if the optical magnification is less or equal to one, and the incident angle or reflection times of the prism can be changed to adjust the measurement resolution according to the user's need.

From Fig. 1, the surface height between two points in an interval Δx is given as

$$\Delta h = \Delta x \alpha, \tag{1}$$

where α is the height gradient in the x-direction, and the reflected light deflects at an angle 2α from the incident light. Let the deflected light be incident into a parallelogram prism at the nearby critical angle. The light, twice reflected in the prism as shown in Fig. 2, has a reflectance given as $R_{\rm s}^2 = R_{\rm s2}$, where $R_{\rm s}$ is the reflectance of the s-polarized light after one reflection. The reflectance curve $R_{\rm s2}$ versus the incident angle θ is shown in Fig. 3. Therefore, the reflectance is inversely proportional to the incident angle θ at the nearby critical angle. Let two adjacent light rays be parallel and normally incident to two points of the specimen, respectively. If there is a small surface height between the two points, the deflection angles are given as

$$2\alpha_1 = 2{\rm d}h_1/{\rm d}x \tag{2}$$

and

$$2\alpha_2 = 2{\rm d}h_2/{\rm d}x \tag{3}$$

respectively, and the deviation angles from the initial incident angle are $\Delta\theta_1 = 2\alpha_1$ and $\Delta\theta_2 = 2\alpha_2$, respectively, where ${\rm d}h_1/{\rm d}x$ and ${\rm d}h_2\ /{\rm d}x$ are the slope of the points in the x-axis at $h(x_1) = h_1$ and $h(x_2) = h_2$, respectively.

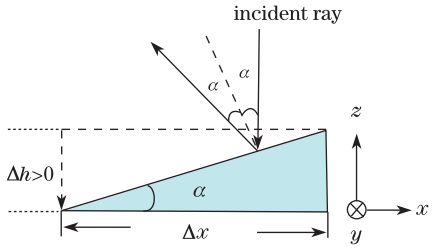

Fig. 1. Ray reflected from an incline plane.

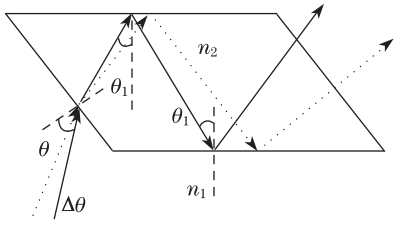

Fig. 2. Ray reflected twice in the parallelogram prism.

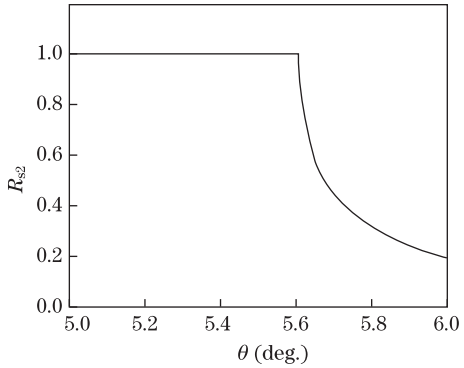

Fig. 3. Reflectance curve of R_{s2} versus the incident angle θ.

The initial incident angle θ_0 is the angle at which the ray reflects from the first point on the x-axis and then incident into the prism. Thus, the reflectance difference ΔR_{s2} [$\Delta R_{s2} = R_{s2}(\theta_2) - R_{s1}(\theta_1)$] between the two angles is inversely proportional to the difference $\theta_2 - \theta_1$ and the surface height $\Delta h = h_2 - h_1$, where $\theta_2 = \theta_0 + \Delta\theta_2$ and $\theta_1 = \theta_0 + \Delta\theta_1$. The surface height is expressed as

$$\Delta h = \Delta R_{s2} \cdot M, \tag{4}$$

where M is the transfer constant. The image system is afocal and consists of two lenses (O2 and L3), a polarized beam-splitter (PBS), and a CCD to increase optical magnification (Fig. 4). The optical transverse magnifiycation M_T is equal to the value of f_3/f_{O2}, where f_{O2} and f_3 are the focal lengths of lenses O2 and L3, respectively. The deviation angle $\Delta\theta$ decreases to the value of $2\alpha/M_T$. Thus, the transfer constant M is given as

$$M = \frac{f_3}{2mf_{O2}}\Delta x, \tag{5}$$

where R_{s2} is the average slope, $m = \Delta R_{s2}/\Delta\theta$, is negative if $\alpha > 0$. Therefore, the transfer constant is dependent on the optical magnification M_T and the slope of the reflectance m; i.e., $M < 0$. From Eqs. (4) and (5), the surface height proportional to the reflectance and is given as

$$h(x,y) = \int \mathrm{d}h = \int M\mathrm{d}R_{s2} = MR_{s2}(x,y) + h_0, \tag{6}$$

where h_0 is the initial height on the surface at the initial incident angle $\theta = \theta_0$.

The experimental setup is shown in Fig. 4, where a beam from a He-Ne laser with a 632.8-nm wavelength is incident to an isolator and then to a beam expander (consisting of an objective O1, a pinhole, and a lens L1), and a polarizer P(0°). The transmission axis of the polarizer is parallel to the x-axis. The isolator is used to prevent the light from the optical system from returning to the laser. Thus, the light out of the polarizer (P(0°)) is a p-polarized light. If a beam, whose polarization direction with respect to the slow or fast axis of a quarter-waveplate ($W_{\lambda/4}$) is 45°, passes twice, the polarization is rotated 90°; i.e., the p-polarized light becomes an s-polarized light. For this reason, the polarization of the beam reflected from the test surface and passing the quarter-waveplate ($W_{\lambda/4}$) again becomes an s-polarized light. It is then reflected by the PBS and is incident to the angular sensor (a parallelogram prism with a refractive index of 1.51509) at the nearby critical angle. The sensor transforms the deviation angle $\triangle\theta$ (due to the height gradient) into the reflectance variation ΔR_{s2}. The s-polarized light is used because the reflectance slope of the s-polarization is more consistent than that of the p-polarization, making it convenient to calculate the average slope of reflectance. The image system consists of the lenses O2 and L3, PBS, and CCD. The CCD is located at the imaging plane and is used to catch the intensity profile of the image. Two incident angles (the nearby critical angle and the total internal reflection (TIR) angle) of the prism are set and used to catch two images with the CCD. The incident angle is adjusted and changed using a rotation stage (URS 100PP, Newport, USA) with an angular resolution of $2\times10^{-4}(°)$. The reference and the test images are caught at the TIR and the nearby critical angle, respectively. The average reflectance of the reference and test images are set to 1.0 and 0.7, respectively, and the initial angle θ_0 is made equal to the angle at $R_{s2} = 0.7$. In addition, to address the problem of image displacement due to the change in the incident angle from θ_0 to TIR, the CCD is laterally translated at a corresponding distance to superpose all the identical points of the two images. The intensity ratios between the test and the reference images must be calculated at each image point. The reflectance profile is then obtained.

In the current experiment, the specimen, a mirror with $\lambda/20$ roughness, is tested, and an atomic force microscope (AFM) is used to test and verify our method. The transverse magnification M_T is equal to 11.8 and the CCD size is 1024×768 (pixels). The pixel size is 4.65×4.65 (μm) and M=–210 nm. Thus, the lateral resolution is 0.4 μm. The experimental results are shown in Fig. 5. Figure 5(a) displays the results of the proposed method and Fig. 5(b) gives the AFM results. Figure 5(a) is a 3D pattern depicting a section of a test area 400×300 (μm). The average roughness R_{av} for the proposed method and for the AFM are 6 and 10 nm, respectively, whereas the root-mean-square roughness R_{rms} are 7 and 13 nm, respectively. These results are quite close to each other. If the results from the AFM are defined as the standard, the difference between the proposed method's results and those of the AFM may be viewed as the system error. Thus, the system error is about 6 nm. In another case, a grating with 20 lines/mm grooves was tested. The 3D

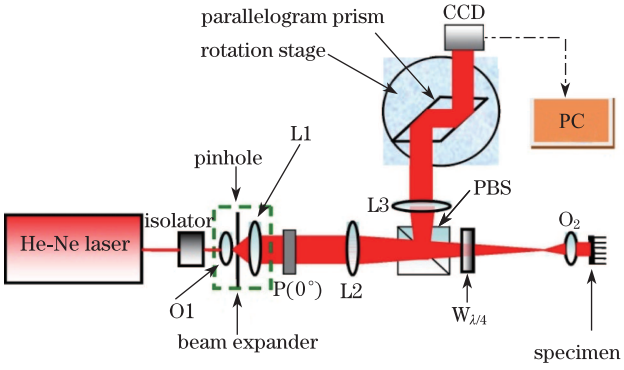

Fig. 4. Experimental setup.

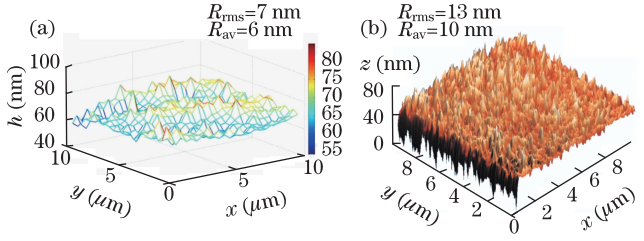

Fig. 5. (a) 3D roughness pattern results and (b) 3D roughness pattern of the AFM results of the mirror with $\ddot{e}/20$ roughness.

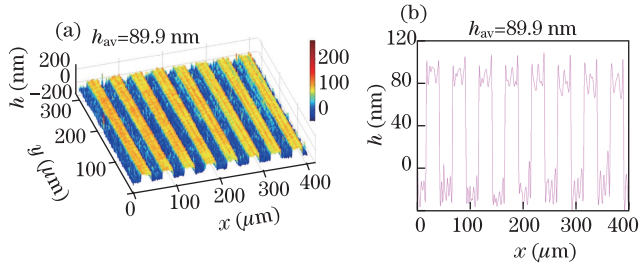

Fig. 6. (a) 3D surface profile pattern of a 20 lines/mm grating; (b) 2D average surface profile pattern of (a).

and 2D profiles are shown in Figs. 6(a) and (b), respectively. The results from another surface profilometer (Dektak-6M, Veeco, USA), which is a contact type profilometer with a tip size of 12.5 μm, are shown in Fig. 7. The resulting average height h_{av} from the proposed method is 89.9 nm, whereas for the Dektak-6M, h_{av}=85.4 nm, with a height difference of 4.5 nm and an error of about 5%. These results are again very close to each other. For the 0–255 gray levels of CCD (8-bits A/D converter), the minimum variation percentage of R_{s2} is 1/256. Thus, the error percentage of the height is 0.4%. From Eq. (6), the height resolution is given as

$$|\Delta h_{min}| = |M \Delta R_{s2\,min}| . \quad (7)$$

Substituting the values $M = -210$ nm and $\Delta R_{s2\,min} = 1/256$ into Eq. (7), the best height resolution obtained is 0.8 nm. The feasibility of the proposed method is thus demonstrated.

In conclusion, a 3D non-scanning and non-interferometric optical profilometer based on the critical angle method is proposed and verified using AFM. The error between the proposed method and AFM is about 6 nm. For the 11.8 optical magnification, the lateral and axial resolutions are 0.4 μm and 0.8 nm, respectively.

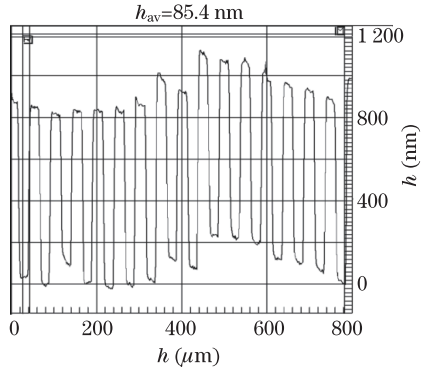

Fig. 7. Surface profile results of a 20 lines/mm grating using Dektak-6M.

The performance is better than that of Dektak-6M. The proposed approach has several advantages, including simplicity, speed, and large area measurement.

This work was supported in part by the NSCT under Grant No. NSC98-2221-E-150-035.

References

1. K. Carlsson, P. E. Danielsson, R. Lenz, A. Liljeborg, L. Majlöf, and N. Åslund, Opt. Lett. **10,** 53 (1985).
2. D. Lin, Z. Liu, R. Zhang, J. Yan, C. Yin, and Y. Xu, Appl. Opt. **43,** 1472 (2004).
3. E. J. Botcherby, M. J. Booth, R. Juškaitis, and T. Wilson, Opt. Lett. **34,** 1504 (2009).
4. E. Vasilyeva and A. Taflove, Opt. Lett. **23,** 1155 (1998).
5. Y. Fainman, E. Lenz, and J. Shamir, Appl. Opt. **21,** 3200 (1982).
6. C. H. Lee, H. Y. Mong, and W. C. Lin, Opt. Lett. **27,** 1773 (2002).
7. G. Li, P. Sun, P. Lin, and Y. Fainman, Opt. Lett. **25,** 1505 (2000).
8. P. de Groot, Appl. Opt. **45,** 5840 (2006).
9. G. Wiegand, K. R. Neumaier, and E. Sackmann, Appl. Opt. **37,** 6892 (1998).
10. S. S. C. Chim and G. S. Kino, Appl. Opt. **31,** 2550 (1992).
11. R. Gauderon and P. B. Lukins, Opt. Lett. **23,** 1209 (1998).
12. T. Kohno, N. Ozawa, K. Miyamoto, and T. Musha, Appl. Opt. **27,** 103 (1988).
13. P. S. Huang and J. Ni, Appl. Opt. **34,** 4976 (1995).
14. C.-T. Tan, Y.-S. Chan, Z.-C. Lin, and M.-H. Chiu, Chin. Opt. Lett. **9,** 011201 (2011).